Int. J. Electrochem. Sci., 13 **(2018)** 11853 – 11866, doi: 10.20964/2018.12.05

International Journal of
ELECTROCHEMICAL
SCIENCE
www.electrochemsci.org

Electrodeposited AuNPs/rGO Nanocomposite as sensor for Cr(VI) Determination in Water

Ye Liu[1], *Guowei Gao*[1,2], *Jingfang Hu*[2,*], *Xiaoping Zou*[2],

[1] Detectation Technology & Automation Equipment, Beijing Information Science & Technology University, Beijing 100192,China
[2] Key Laboratory of sensor, Beijing Information Science & Technology University, Beijing 100101, China
[*]E-mail: jfhu@bistu.edu.cn

Received: 8 May 2018 / *Accepted:* 30 August 2018 / *Published:* 5 November 2018

A facile two-step electrochemical deposition of gold nanoparticles (AuNPs)/reduced graphene oxide (rGO) (AuNPs/rGO) nanocomposite was developed for Cr(VI) determination in water. First, electrodeposition of rGO on GCE by electroreduction of GO using cyclic voltammetry (CV), and then AuNPs were electrodeposited on rGO sheets using CV to obtain as AuNPs/rGO/GCE. The AuNPs/rGO nanocomposite was characterized by scanning electron microscopy (SEM), transmission electron microscopy (TEM) and energy dispersive X-Ray spectroscopy (EDS) analysis. The deposition time, and concentration of HCl supporting electrolyte were respectively optimized for Cr(VI) determination. Square wave voltammetry (SWV) was applied for the detection of Cr(VI). The experimental results demonstrated the AuNPs/rGO/GCE has excellent electrocatalytic ability for Cr(VI) reduction, and a linear range of 0.1 μM-30 μM, with a high sensitivity of 0.79915 μA/μmolL^{-1}, and a detection limit of 0.046 μM (S / N = 3) for Cr(VI) determination. The signal remained 92.98% after 12 h measurement suggested that the AuNPs/rGO nanocomposite has good stability for Cr(VI) determination. The common interfering irons of Mg^{2+}, Zn^{2+}, Cu^{2+}, Mn^{2+} and Cr^{3+} were separately investigated, and less than 2% deviation values were obtained, indicating that the proposed AuNPs/rGO nanocomposite has good selectivity for Cr(VI) determination.

Keywords: Cr(VI) determination; AuNPs/rGO nanocomposite; electrochemical deposition; square wave voltammetry

1. INTRODUCTION

Chromium is one of the most common heavy metal pollutants[1]. It is widely used in metal plating, wood preservation, ink manufacturing, dyes, pigments, glass and ceramics, tanning and textile

industries[2]. Chromium contained in which exhaust gas and industrial wastewater can cause environmental pollution and cause serious health hazards to humans[3]. Cr(III) and Cr(VI) are the two most common valence states of Chromium. Cr(III) is relatively innocuous and an essential micronutrient, but Cr(VI) is highly toxic and its carcinogenicity and toxicity are 100-1000 times higher than that of Cr(III)[4-5]. The World Health Organization (WHO) limit of Cr(VI) in water is 50 μg/L[6]. Therefore, the determination of Cr(VI) in water, especially in low concentration is significantly required.

Many different methodologies and analytical instruments have been used for the determination of Cr(VI) which includes ultraviolet and visible spectrophotometry[7], mass spectrometry[8], chromatographic analysis[9] and fluorescence analysis[10]. All these methods are sensitive, however, there are some problems such as a long detection time, complex operation, high equipment costs which are difficult for field and on-site monitoring. Recently electrochemical methods have been widely used for Cr(VI) detection in water because of its advantages of simple operation, fast detection, environment friendly and convenience for field monitoring. Up to date, some modified electrodes as electrochemical sensors have been successfully applied to Cr(VI) detection. Especially, the introduction of nanomaterials (AuNPs[11], AgNPs[12], carbon nanotubes[13], etc.) into modified electrodes has obvious advantages in improving the sensor performances such as sensitivity, stability and selectivity for Cr(VI) sensing because of their special small size effect, surface effect, physical and catalytical effect. Among them, the noble metal of AuNPs received great interests due to its excellent chemical stability and catalytic property for Cr(VI) reduction. Tsai[14] investigated the voltammetric behavior of Cr(VI) at bare ITO, bulk Au and AuNPs-electrodeposited electrodes, respectively, and found that AuNPs-electrodeposited electrode demonstrated unique catalytic behavior, higher sensitivity and stability in the reduction of Cr(VI). Compton[15] proposed a method of fast detection of Cr(VI) using a AuNPs-plated carbon composite electrode, and a detection limit of 4.4 μg/L was obtained without any accumulation process. Ouyang[16] prepared a flower-like self-assembly of AuNPs modified electrode using two-step method of electroplation and self-assembly for Cr(VI) detection, resulting a good performance of stability, reproducibility and linearity in a low-level concentration range of 10-1200 ng/L. While a good catalytic activity and stability for Cr(VI) reduction, the practical application of the single AuNPs material is limited due to their aggregation during preparation process, the interference from other heavy metal ions (Cu(II)[17], Pb(II)[18], etc.) and high cost of the rare material[19]. It is thus highly desirable to develop a sensor that is not only sensitive but also reliable, selective, and economical in its practical application for Cr(VI) measurement.

Graphene is a novel carbon nanomaterial with a two-dimensional honeycomb network structure formed by the sp^2 hybridization of carbon atoms. It has attracted extensive research attention for decades due to its large specific surface area, unique electronic, catalytic, sensing properties, as well as good chemical stability, good compatibility with other nanomaterials or biomaterials, and ultra-high carrier mobility[20-23]. The methods for preparation of graphene mainly include micro mechanical peeling[24], SiC epitaxial growth[25], chemical vapor deposition[26], chemical synthesis[27], etc., however, these methods require complicated processes, expensive costs, and toxic reagents. Therefore, it is of great interest to look for a simple and environment-friendly method for the preparation of graphene sheets. The electrochemical method is the most controllable for preparation of nanomaterials,

in which the size, density, morphology and performance can be well-controlled by setting the parameters of potential, time, pH, and concentration etc. It is worthy mentioned that the electrochemical method is also useful in the preparation of graphene through electrochemical reduction of graphene oxide (GO) into reduced graphene (rGO) without any reducing agents under room-temperature condition. In addition, rGO prepared by electrochemical reduction can also preserve partial oxygen-containing functional groups on rGO sheets. More importantly, it was found that the residual oxygen-containing functional groups of epoxy (C-O), hydroxyl (-OH) on rGO sheets can enhance the adsorption ability of seizing Cr(VI) on electrode surface, which, correspondingly, would be great helpful in improving the electrode selectivity for Cr(VI) sensing[28-29].

In recent years, rGO-metal nanocomposites are emerging as a class of exciting materials in sensor development. It has been revealed that the residual oxygen-containing functional groups on rGO can contribute to the nucleation and growth of metal nanoparticles on the surface of rGO sheets and the large specific surface area of rGO sheets can prevent the aggregation of metal nanoparticles[30-32]. So when incorporated into metal nanomaterials, rGO can remarkably improve the properties of these host metal nanomaterials. Herein, we develop a new and facile two-step electrochemical deposition (electrodeposition) approach to fabricate a novel AuNPs/rGO nanocomposite for Cr(VI) determination. In this two-step electrodeposition route, the electrodeposition of rGO and AuNPs are carried out sequentially, generating AuNPs on the surface of rGO sheets. Favorably, compared with single rGO or AuNPs, this new AuNPs/rGO nanocomposite possess the advantage of the above-mentioned rGO and AuNPs which presents enhanced electrocatalytic performance for Cr(VI) reduction. The as-prepared AuNPs/rGO nanocomposite showed high sensitivity, low detection limit, good selectivity and excellent stability for Cr(VI) determination in water.

2. EXPERIMENTAL

2.1 Chemicals and reagents

4 mg/mL graphene oxide (GO) solution was purchased from Graphenea. Chloroauric acid ($HAuCl_4$) was purchased from Sigma. Potassium ferricyanide ($K_3[Fe(CN)_6$) and potassium dichromate (K_2CrO_4)were purchased from Sinopharm Chemical Reagent Co. Ltd (Beijing china). Different concentrations of Cr(VI) standard solution were dilute from 3000 μM standard stock solution (0.1 M of HCl as the supporting electrolyte). Sodium hydroxide (NaOH), potassium chloride (KCl), concentrated hydrochloric acid (HCl, 37%), chromium nitrate ($Cr(NO_3)_3$), magnesium sulfate heptahydrate ($MgSO_4 \cdot 7H_2O$), manganese sulphate ($MnSO_4$), copper(II) sulfate pentahydrate ($CuSO_4 \cdot 5H_2O$), Zinc nitrate hexahydrate ($Zn(NO_3)_2$) were purchased from Xilong Chemical Co. Ltd (Guangxi, China). All other chemicals were of analytical grade and used without further purification. All solutions were prepared in deionized water.

2.2 Instrumentation

All electrochemical experiments were performed using a CHI660E electrochemical analyzer (Shanghai Chenhua Instruments). Ultrasonic cleaning equipment from Shenzhen Jie Union Cleaning Co., Ltd. The system consisted of GCE working electrode, an Pt counter electrode, and a commercial saturated Ag/AgCl electrode (CRE). Scanning electron microscope (SEM) analysis was got on SIGMA field emission scanning electron microscope produce by Zeiss. Transmission electron microscope (TEM) analysis was got on JEM-1200EX transmission electron microscope by Japan JEOL company. energy dispersive X-Ray spectroscopy (EDS) analysis was got on JSM-7500F.

2.3 Electrodeposition of AuNPs/rGO nanocomposite

The GCE and platinum electrode were polished on the suede with Al_2O_3 powder until a mirror like surface was obtained. After polishing, they were respectively subjected to ultrasonic cleaning with acetone, ethanol and deionized water for 5 minutes. Finally, they were rinsed with ultrapure water and blown dry with nitrogen. A graphene oxide solution was prepared at a concentration of 2.0 mg/mL, containing KCl at a concentration of 0.1M as a supporting electrolyte. The rGO was deposited by cyclic voltammetry with the scan range of -1.5-0.5 V, the scan rate of 40 mV/s and the deposition time of 500 s. The rGO/GCE was placed in deionized water for 3 to 5 times to remove adsorbed GO and potassium chloride. Next, the rGO/GCE was placed in 1 mM $HAuCl_4$ solution containing 0.1 M KCl, and AuNPs was deposited on the rGO surface by cyclic voltammetry with a scan range of -0.5-0.3 V, scan rate of 50 mV/s, deposition time of 192s. Finally, the AuNPs/rGO/GCE is pulled in deionized water for 3 to 5 times to remove the surface impurities and placed in deionized water for preservation. This electrode is now ready for further application in the determination of Cr(VI).

2.4 Electrochemical measurement for Cr(VI) determination

The GCE modified with AuNPs/rGO nanocomposite was put into aqueous solution containing 0.1 M HCl and Cr(VI) with different concentrations. The determination of different Cr(VI) concentration was performed using square-wave voltammetry (SWV). The potential range was set to be 0.6 V to -0.2 V with a scan frequency of 15 Hz.

3. RESULTS AND DISCUSSION

3.1 Characterization of AuNPs/rGO nanocomposite

The morphology of the electrodeposited AuNPs/rGO nanocomposite was characterized by SEM and TEM. Fig. 1A shows the SEM image of the surface morphology of rGO/GCE prepared in the first step. It can be seen that obviously typical wrinkled sheet structure of graphene, indicating that the GO sheets were successfully electroreduced to rGO sheets on electrode surface. After the

electrodeposition of AuNPs on rGO/GCE, the SEM image of the prepared AuNPs/rGO nanocomposite was shown in Fig. 1B. It can be observed that the nanoparticles with a diameter of about 100 nm-400 nm (shown in the bottom-right insert) on the rGO sheets, and the nanoparticles are evenly distributed on rGO surface, which suggests that the AuNPs were successfully electrodeposited on rGO surface.

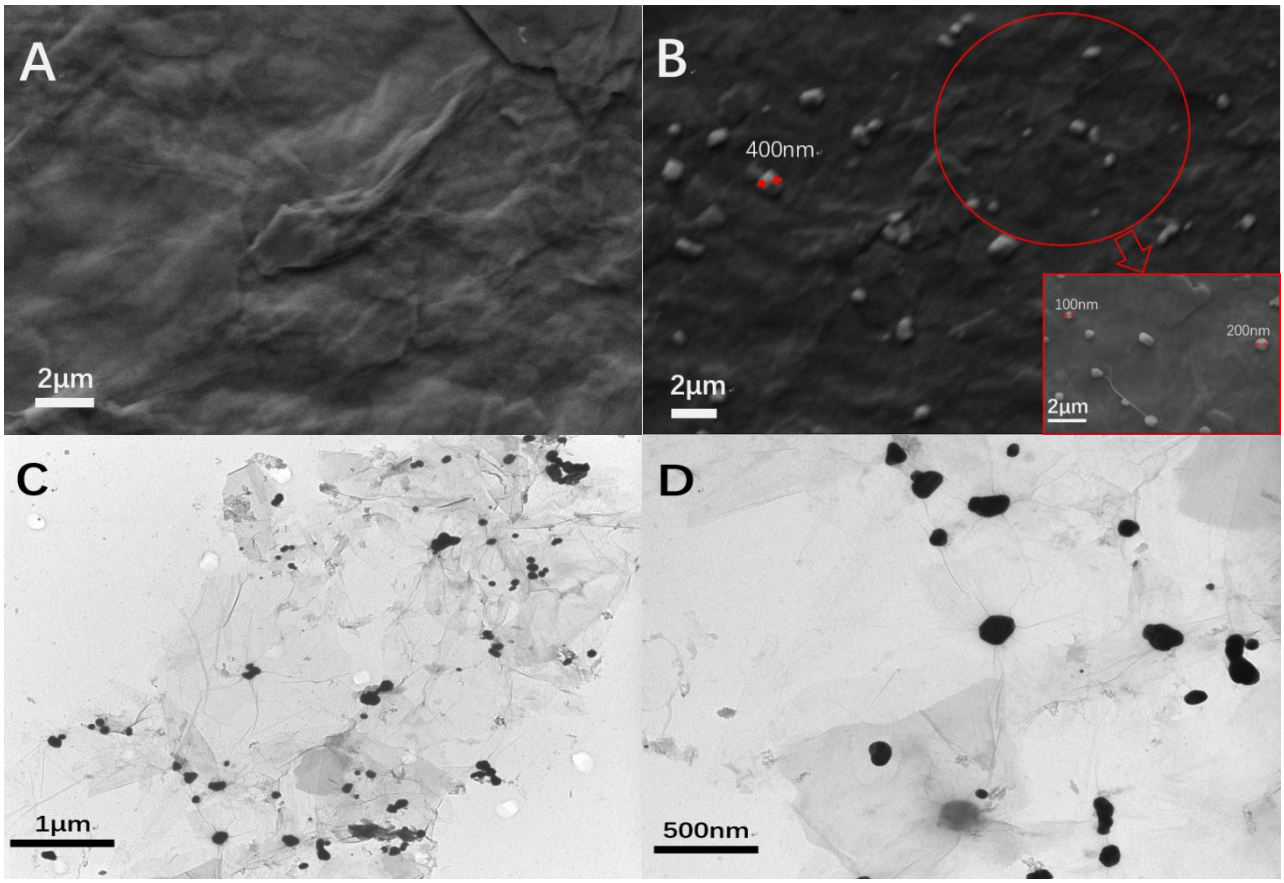

Figure 1. (A) SEM image of rGO/GCE; (B) SEM image of AuNPs/rGO/GCE (the inset is the corresponding partial enlargement of B); (C) TEM image of 25000 magnification of AuNPs/rGO/GCE; (D) TEM image of 60000 magnification of AuNPs/rGO/GCE.

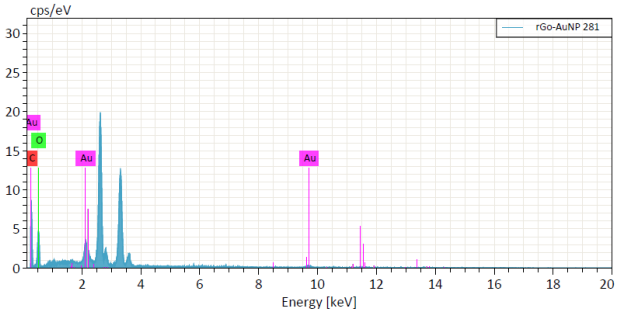

Figure 2. EDS spectrum of AuNPs-rGO

Through the TEM images, the single layer structure of graphene was observed in Fig. 1C and D, most importantly, it can be seen that the AuNPs are homogeneously distributed on rGO sheets.

Elemental compositions of the prepared AuNPs/rGO nanocomposite were observed by energy dispersive spectrum (EDS) (Fig. 2**)**. Signature peaks of Au, C and O were observed for AuNPs/rGO, where the presence of O represented the residual oxygen-containing functional groups of rGO. The results indicates that Au and rGO can both be successfully electrochemically synthesized under the given conditions.

3.2 Optimization

3.2.1 Effect of deposition time

Deposition time is a key factor for the density, shape and properties of the deposited nanomaterials. So the deposition time of two-step electrodeposition of rGO and AuNPs was optimized respectively. The electrochemical method of cyclic voltammetry (CV) was used for the electrodeposition of rGO/AuNPs nanocomposite. The electrodeposition time increases along with increasing the CV scanning cycles. In the first step of electrodeposition of rGO on GCE in a potential range of -1.5-0.5 V, the deposition time of 100 s (2 cycles), 300 s (6 cycles), 500 s (10 cycles), 600 s (12 cycles), 700 s (14 cycles), and 800 s (16 cycles) were orderly selected for rGO deposition. Then the electrochemical activity of the prepared rGO/GCE modified electrodes were sequentially investigated in 1 mM potassium ferricyanide solution and the results were shown in Fig. 3A and B. It is illustrated from Fig. 3A that the current responses increased with the increase of electrodeposition time from 100 s to 500 s, but decreased when the deposition time is more than 500 s. The reduction peak current values were also recorded as shown in Fig. 3B, from which the peak current quickly increases with deposition time increasing from 100s to 500 s, but deceases from 500 s to 700 s, and maintains a low level when the deposition time increased over 700 s. The reason is considered that the deposited rGO sheets ceaselessly aggregated layer-by-layer with an increase of deposition time due to their strong π-π interaction, which the electron transfer rate on the electrode surface can be effectively increased and the current response can be enhanced. However, when the deposited rGO layer arrivals a certain thickness, the diffusion of electrons on the modified electrode surface will be hindered, resulting the corresponding drop of the electrode activity and the response current[33-35]. Therefore, 500 s was the optimal position time for rGO modification on GCE in the first step.

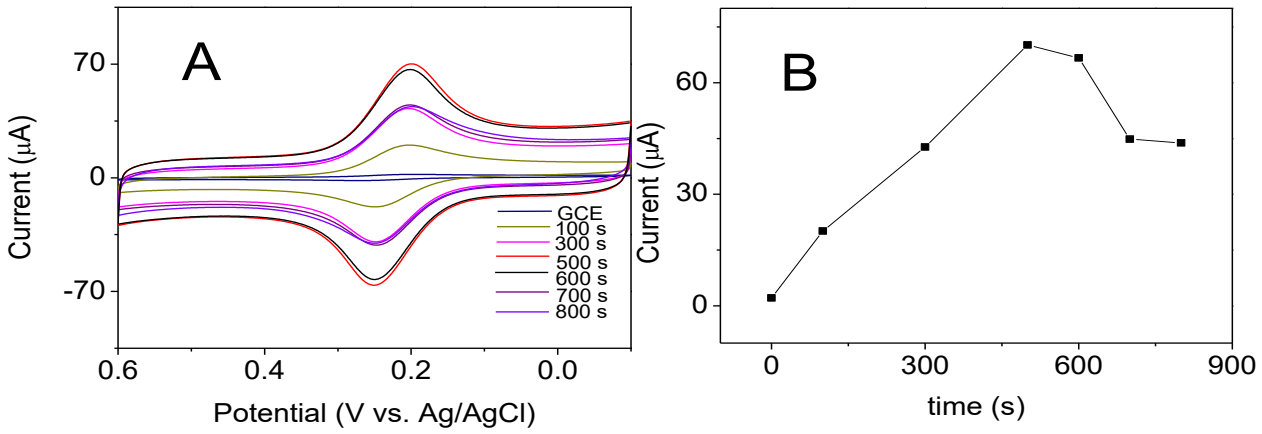

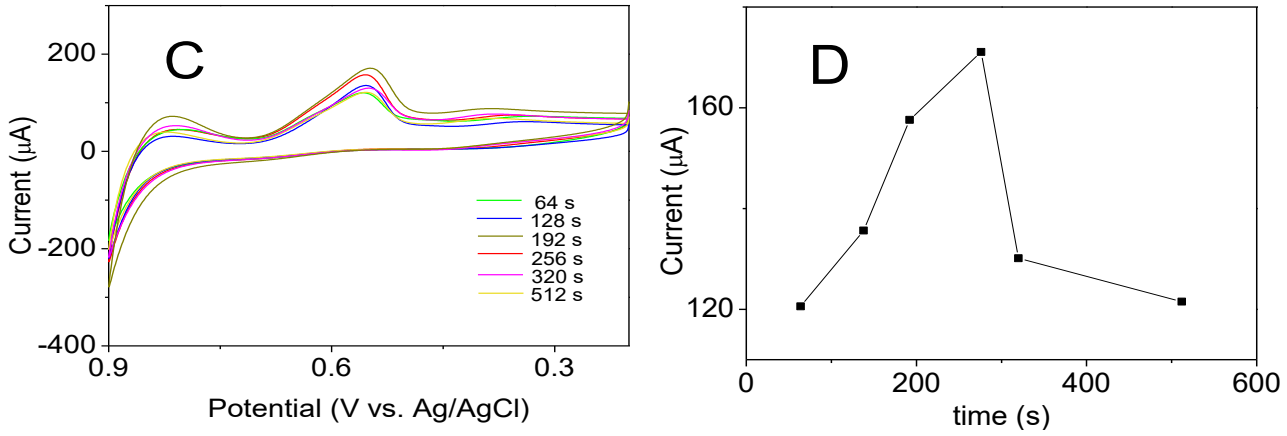

Figure 3. (A) CV curves of rGO/GCE modified electrodes obtained with different deposition time from 0 s to 800 s in 1mM potassium ferricyanide solution. (B)The relationship between the reduction peak current and the deposition time for rGO preparation. (C) CV curves of 10 μM Cr(VI) standard solution on AuNPs/rGO/GCE modified electrodes. (D) The relationship between the reduction peak current and the deposition time for AuNPs preparation.

In the second step of electrodeposition of AuNPs on rGO/GCE in a potential range of -0.5-0.3 V, the electrodeposition time of 64 s (2 cycles), 128 s (4 cycles), 192 s (6cycles), 256 s (8 cycles), 320 s (10 cycles) and 512 s (16 cycle) were orderly selected for AuNPs deposition. Then the electrochemical activity of the prepared AuNPs/rGO/GCE modified electrodes were sequentially investigated in 10 μM Cr(VI) standard solution and the results were shown in Fig. 3C and D. From Fig. 3C, the current responses increase with the increase of deposition time from 64 s to 192 s, but decrease when the deposition time is more than 192 s. The reduction peak current values were also recorded as shown in Fig. 3D, from which the peak current quickly increase with deposition time increasing from 64 s to 192 s, but decease from 192 s to 512 s, and maintain a low level when the deposition time increased over 320 s. The reason is speculated that the synergistic catalysis effect of AuNPs and rGO for Cr(VI) reduction is gradually improved along with the amount of electrodeposited AuNPs increasing on rGO sheets, which correspondingly resulted increased current response[36-37]. Nevertheless, when the deposition time increased up to a certain point of 192 s, a large number of AuNPs densely covered on the rGO layer, which would cause reduced oxygen-containing functional group of rGO exposed towards sample solution for sizing Cr(VI), thus weakening the synergistic catalytic effect of AuNPs and rGO for Cr(VI) reduction. Therefore, 192 s is the optimal deposition time for AuNPs preparation

3.2.2 Effect of HCl concentration

According to previous researches, acid solution is more suitable for electrochemical reduction of Cr (VI)[38-39]. That is because, only in acidic condition, the anionic specie of $HCrO_4^-$ is the predominant in solution, which possess a perfect electrochemical activity. The influence of different supporting electrolytes (HCl, H_2SO4 and HAC) to the rate of Cr(VI) reduction has been investigated and it has been demonstrated that HCl is the best supporting electrolyte for Cr (VI) reduction. So HCl

was used as the supporting electrolyte for Cr (VI) determination in this experiment. It is well known from the literature[40] that the variation of H^+ concentration can interfere in the chemical equilibrium of Cr (VI) in aqueous solution. Therefore, it is necessary to optimize the HCl concentration for Cr (VI) determination.

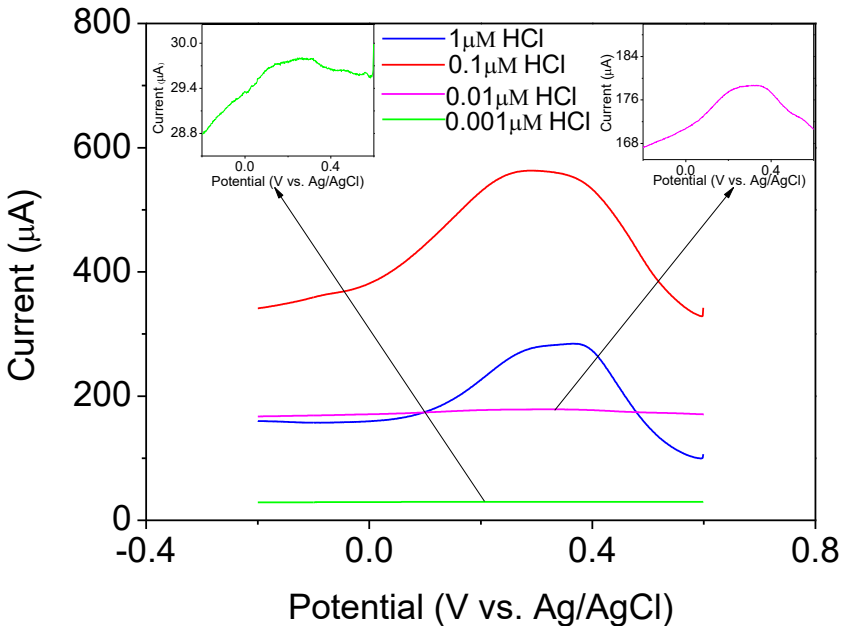

Figure 4. SWV curve of 10 μM Cr(VI) on AuNPs/rGO/GCE in different concentrations of HCl supporting electrolyte (1 M, 0.1 M, 0.01 M and 0.001 M). SWV detection conditions: step potential, 1 mV; amplitude, 25 mV; frequency, 15 Hz.

HCl supporting electrolytes with different concentrations of 1 M, 0.1 M, 0.01 M, and 0.001 M was estimated for 10 μM Cr(VI) electroreduction using SWV method over the -0.2-0.6 V range. As shown in Fig. 4, the peak current increased with the increase of HCl concentration from 0.001 M to 0.1 M, but decreased when HCl concentration is more than 0.1 M. The reason is thought that the electrochemical reduction of Cr(VI) is more efficient due to the dominate $HCrO_4^-$ with increase of the concentration of H^+ , but when the concentration of HCl continues to increase up to 1 μM, Cl^- concentration would interferes with the electrocatalytic reduction of Cr(VI) and the current response correspondingly decreases[41].

3.3 Electrocatalytic reduction of Cr(VI)

In order to investigate the electrocatalytic ability for Cr(VI) reduction, different modified electrodes of rGO/GCE, AuNPs/GCE and rGO/AuNPs/GCE were prepared separately under the same electrodeposition conditions. SWV method was used for electrochemical reduction of Cr(VI) as shown in Fig. 5. It can be observed that the bare GCE did not show any reduction peak between the selected potential window, but AuNPs, rGO and AuNPs/rGO nanocomposite possess obvious reduction peaks presented at about 0.3 V, suggesting that the electrodeposited AuNPs, rGO and AuNPs/rGO

nanocomposite all have electrocatalytic ability for Cr(VI) reduction. It also can be seen that the peak current of rGO/GCE is obviously higher than AuNPs/GCE. The possible reasons can be analyzed from two points. On one hand, the rGO possesses larger specific surface area which can speed up the electronic transfer rate. On the other hand, the adsorption capacity of the oxygen-containing functional group on rGO sheets to Cr(VI) can seize more Cr(VI) on electrode surface. Just as we thought, the reduction peak of AuNPs/rGO/GCE is higher than other modified electrodes of AuNPs/GCE and rGO/GCE, indicating that there are a synergistic effect between AuNPs and rGO for electrocatalytic reduction of Cr(VI). In addition, the reduction potential on AuNPs/rGO/GCE was shifted to left comparing with AuNPs/GCE and rGO/GCE, revealing that the composite of AuNPs and rGO can improve the electron transfer rate of Cr(VI) reduction. So the prepared AuNPs/rGO nanocomposite has an excellent electrocatalytic ability for Cr(VI) reduction and it is potential for the further application in Cr(VI) determination.

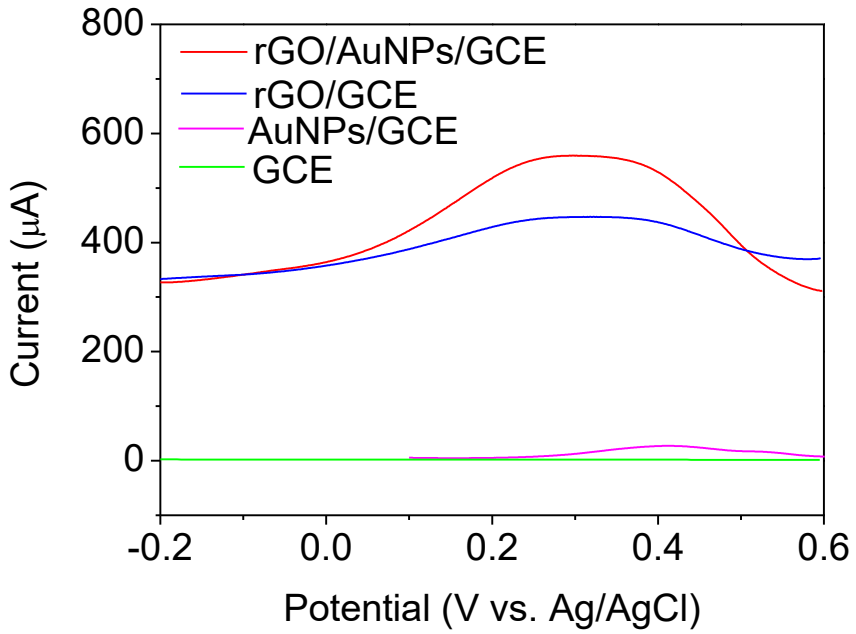

Figure 5. SWV curves on bare GCE and the modified electrodes of rGO/GCE, AuNPs/GCE and rGO/AuNPs/GCE in 1 μM Cr(VI) standard solution. Other conditions, as in Fig. 4.

3.4 Electrochemical determination of Cr(VI)

Electrochemical determination of Cr(VI) was carried out by SWV using the prepared rGO/AuNPs/GCE. As shown in Fig. 6, it can be seen that the response current increases with the concentration increases, and there is a good linear relationship between the reduction peak current and the concentration of Cr(VI) over the range of 0.1 μM-30 μM with a high sensitivity of 0.79915 $\mu A/\mu molL^{-1}$ and correlation coefficient of 0.97616. From the linear equation of the plot, the limit of detection (LOD) was estimated 0.046 μM according to S/N = 3. In order to have a good comparison between the prepared rGO/AuNPs/GCE with other reported modified electrodes for Cr(VI) determination, some of their performances were summarized in Table 1. It is found that the linearity

dynamic range and limit of detection obtained for the prepared sensor in this research seems to be superior to other reported Cr(VI) sensor electrodes, which may be contributed to the excellent synergistic effect of rGO and AuNPs for catalytic reduction of Cr(VI). The linear correlation coefficient is 0.97616, however, which is not so high compared with other sensing electrodes. The further data analysis of the linear relationship was conducted for the different concentration ranges of 1~10 μM (Fig.7A), 1~20 μM (Fig.7B), and 0.1~10 μM (Fig.7C). It is found that the highest correlation coefficient of 0.999 was obtained between the reduction peak current and the Cr(VI) concentration in the range from 1 μM to 10 μM. The results suggests that the proposed sensing electrode may be better for the application of Cr(VI) measurement in low concentration from 1 μM to 10 μM.

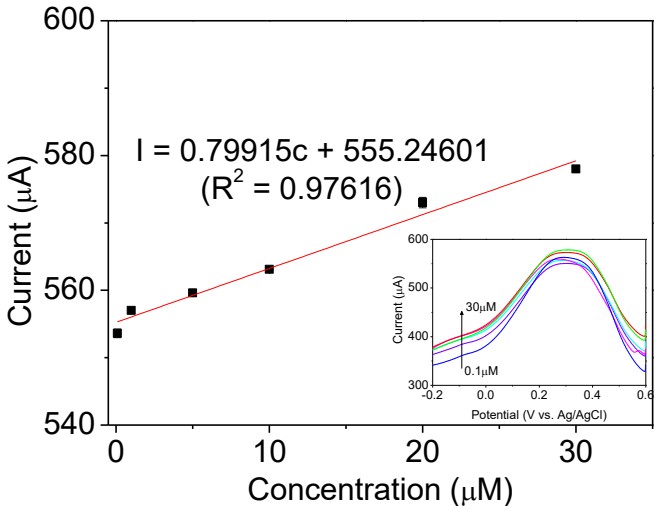

Figure 6. The linear relationship between current response and concentration from 0.1 μM to 30 μM. Inset. corresponding SWV curves is shown. Other conditions, as in Fig. 4.

Table 1. Comparison of the prepared electrode with other reported Cr(VI) electrode.

Modified electrode	Linear range (μM)	correlation coefficients	Detection limit (μM)	Reference
Indium tinoxide electrode modified with AuNPs	0.5~50	0.998	0.1	[14]
Indium tinoxide electrode modified with agar/polyaniline film	2.48~50	0.995	2.48	[42]
GCE modified with AgNPs/Nafion film composite material	0.038~4.420	0.996	0.0128	[43]
Mercury electrode modified with Cu-adenine complex	0.1~2.3	0.998	0.04	[44]
Screen-printed electrode modified with L-3,4-dihydroxyphenylalanine	0.19~2.4	0.990	0.11	[45]
GCE modified with AuNPs/rGO nanocomposite	0.1~30	0.976	0.046	This work

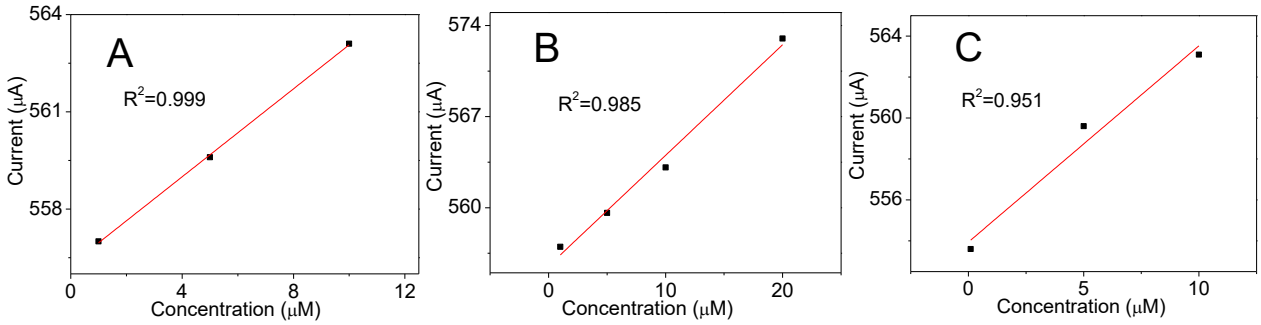

Figure 7. The linear relationship between current response and concentration from (A) 1μM to 10μM; (B) 1μM to 20μM; (C) 0.1μM to 10μM.

3.5 Selectivity , repeatability and stability

In general, in the practical measurement of Cr(VI) in real water samples, the common heavy metal interference ions in surface water are Mn^{2+}, Cu^{2+}, Mg^{2+}, Ag^{+}, Cd^{2+}, Ni^{2+}, $Zn^{2+}$and Cr^{3+} etc. So the selectivity of the rGO/AuNPs/GCE modified electrode was evaluated by monitoring the current response in the presence of other heavy metal ions including Mn^{2+}, Cu^{2+}, Mg^{2+}, Zn^{2+} and Cr^{3+} at the concentration of 1 μM Cr(VI). The peak current values were recorded with the addition of 10-fold concentration of Mg^{2+} , Zn^{2+} , Cu^{2+} , Mn^{2+} and 100-fold concentration of Cr^{3+} to the 1 μM of Cr(VI) standard solution respectively. The results were shown in Table 2. It is found that, the common interfering ions of Mg^{2+} , Zn^{2+} , Cu^{2+} , Mn^{2+} and Cr^{3+} were separately investigated, and less than 2% deviation values were obtained, suggesting that the proposed AuNPs/rGO nanocomposite has good selectivity for Cr(VI) determination.

Table 2. Current deviations found for the addition of various metallic ions.

Interfering ions added	concentration (μM)	Deviation (%)
Cr^{3+}	100	0.53
Zn^{2+}	10	0.18
Mn^{2+}	10	0.54
Mg^{2+}	10	0.35
Cu^{2+}	10	1.06

The repeatability of the AuNPs/rGO/GCE was evaluated by performing 12 repeated voltammetric measurements in 1 μM of Cr(VI) standard solution using the same modified electrode, and the maximum error of the reduction peak current values of 12 measurements is only 2.1% (data not shown), so the modified electrode has good repeatability. In order to further estimate the stability of the AuNPs/rGO/GCE, SWV measurement of 1 μM Cr(VI) was performed at regular interval (2 h) over a period of 12 h. As shown in Fig. 7, the obtained reduction peak current value remained 92.98% after 12 h measurements which indicated that the AuNPs/rGO nanocomposite has good stability for Cr(VI) determination.

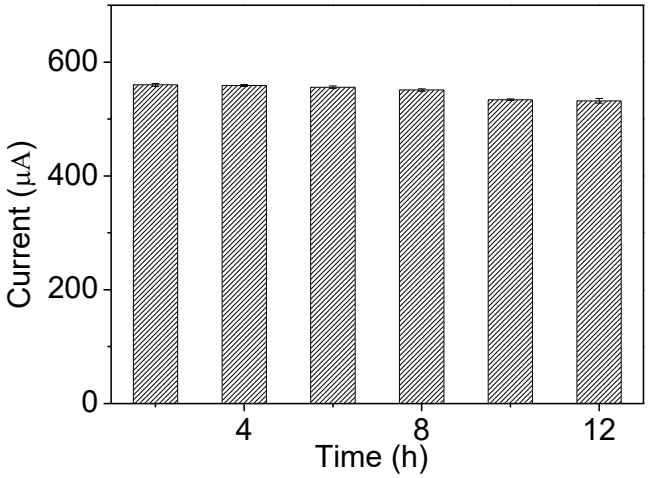

Figure 7. Stability of AuNPs/rGO/GCE towards Cr(VI) (1μM Cr(VI) standard solution). Other conditions, as in Fig. 4.

3.6 Determination of Cr(VI) in water sample

The proposed sensor was used for analysis of Cr(VI) levels in real water samples collected from 5 different lakes and rivers around Beijing. No Cr(VI) can be detected in the original water samples. Therefore, a detection test was performed by introducing known concentration of Cr(VI) into the water sample in order to verify the feasibility of this sensor in real water determination. The experimental results are collected in Table 3, and the percentages of recovery higher than 93%. It must be emphasized that 0.1 M HCl were introduced into each water sample.

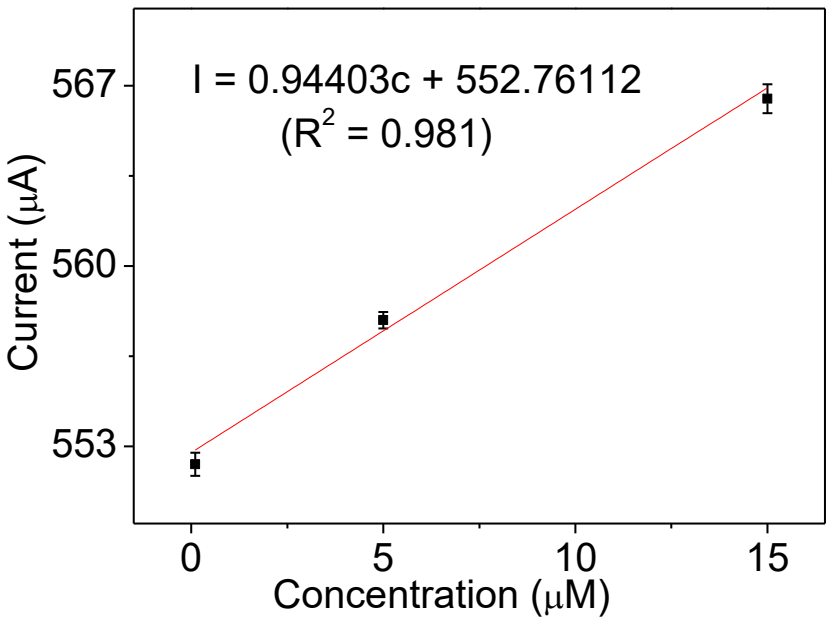

Figure 8. The calibration curve of Cr(VI) in water samples

Table 3. Determination of Cr(VI) in several water samples

Water sample	**Cr(VI) added** (μM)	**Cr(VI) found after addition** (μM**)**	**Recovery**(%)
Sample 1	0.5	0.56	112
Sample 2	1	1.14	114
Sample 3	5	4.67	93.4
Sample 4	8	8.61	107.6
Sample 5	10	10.13	101.3

4. CONCLUSIONS

In this paper, a novel and facile two-step electrodeposition method was employed for the preparation of AuNPs/rGO nanocomposite for Cr(VI) determination in water. The electrodeposited rGO sheets enhanced the effective surface area and acted as a good support for AuNPs growth. It was found there are obvious synergistic effect between AuNPs and rGO for electrocatalytic reduction of Cr(VI). The AuNPs/rGO nanocomposite modified electrode showed a high sensitivity of 0.79915 $\mu A/\mu molL^{-1}$ and low detection of 0.046 μM. The response of the modified electrode towards Cr(VI) is linear from 0.1 μM up to 30 μM. Additionally, the selectivity, repeatability and stability were demonstrated good for Cr(VI) determination. All of the above results indicate that the AuNPs/rGO nanocomposite modified electrode modified electrode holds promise for practical detection in the future.

ACKNOWLEDGEMENT
This work was supported by the National Natural Science Foundation of China (NO. 9011610902), and Science and Technology Project of Beijing Educational Committee (NO. KM201611232021).

References

1. S. Mahiya, G. Lofrano and S. K. Sharma, *J. Chem.,* 3 (2014) 132.
2. S. M. Rosolina, S. A. Bragg, R. Ouyang, J. Q. Chabeis and Z. L. Xue, *J. electronal. Chem.*, 781 (2016) 120.
3. B. Dhal, H. N. Thatoi, N. N. Das, and B. D. Pandey, *J. Hazard. Mater*., 250-251 (2013) 272.
4. C. Santhosh, M. Saranya, R. Ramachandran, S. Felix, V. Velmuragan and A. N. Grace, *Journal of Nanotechnology*, 2014(2014):7.
5. M. Dakiky, M. Khamis, A. Manassra and M. Mer'eb, *Adv. Environ. Res.*, 6 (2002) 533.
6. WHO, Guidance for Drinking Water Quality: Recommendations, vol. 1, World Health Organization, Geneva, Switzerland, 3rd edition, 2008.
7. T. G. Levitskaia, M. J. O'Hara, S. I. Sinkov and O. B. Egorov, *Appl. Spectrosc.*, 62 (2008) 107.
8. A. P. Maichand, K. A. Kumar, H. Chong, S. M. Blair and J. S. Brodbelt, *Anal. Chem.,* 72 (2000) 2433.
9. T. Williams, P. Jones and L. Ebdon, *J. Chrommatogr. A*, 482 (1989) 361.
10. L. Wang, T. Xia, J. Liu, L. Wang, H. Chen, L. Dong and G. Bian, *Spectrochim. Acta. A* 62 (2005) 565.
11. B. Liu, L. Lu, M. Wang and Y. Zi, *J. Chem. Sci.*, 120 (2008) 493.
12. H. D Nguyen, T. T. L. Nguyen, K. M. Nguyen, T. A. T. Tran, A. M. Nguyen and Q. H. Nguyen, *AJAC*., 6 (2015) 457.

13. A. Deep, A. L. Sharma, S. K. Tuteja and A. K, Paul, *J. Haz. Mat.*, 278 (2014) 559.
14. M. C. Tsai and P. Y. Chen, *Talanta*, 76 (2008) 533.
15. R. T. Kachoosangi and R. G. Compton, *Sens. Actuators B Chem.*, 178 (2013) 555.
16. R. Ouyang, S. A. Bragg, J. Q. Chambers and Z. L. Xue, *Anal. Chim. Acta*, 722 (2012) 1.
17. D. Peng, B. Hu, M. Kang, M. Wang, L. He, Z. Zhang and S. Fang, *Appl. Supf. Sci.*, 390 (2016) 422.
18. S. A. Tukur, N. A. Yusof and R. Hajian, *IEEE Sens. J.*, 15 (2015) 2780.
19. N. Khlebtsov and L. Dykman, *Chem. Soc. Rev.*, 42 (2011) 1647.
20. H. K. Chae, D. Y. Siberio-Perez, J. Kim, Y. Go, M. Eddaoudi, A. J. Matzger, M. O'Keeffe and O. M. Yaghi, *Nature*, 427 (2014) 523.
21. X. U. Chao, X Wang and J Zhu, *J. Phys. Chem. C*, 112 (2008) 19841.
22. X. Kang, J. Wang, H. Wu, I. A. Aksay, J. Liu and Y. Lin, *Biosens. Bioelectron.*, 25 (2009) 901.
23. K. S. Novoselov, A. K. Geim, S. V. Morozov, D. Jiang, Y. zhang, S. V. Dubonos, V. Grigorieva and A. A. Firsov, *Science*, 306 (2004) 666.
24. C. Knieke, A. Berger, M. Voigt, R. N. K. Taylor, J. Rohrl and W. Peukert, *Carbon*, 48 (2010) 3196.
25. C. Berger, Z. Song, X. Li, X. Wu, N. Brown, C. Naud, D. Mayou, T. Li, J. Hass, A. N. Marchenkov, E. H. Conrad, P. N. First and W. A. Heer, *Science*, 312 (2006) 1191.
26. K. S. Kim, Y. Zhao, H. Jang, S. Y. Lee, J. M. Kim, K. S. Kim, JH. Ahn, P. Kim, JY. Choi and B. H. Hong, *Nature*, 457 (2009) 76.
27. C. D. Sippson, J. D. Brand, A. J. Berresheim, L. Przybilla, H. J. Räder and K. Müllen, *Chem. Eur. J.*, 8 (2002) 1424.
28. H. L. Guo, X. F. Wang, Q. Y. Qian, F. B. Wang and X. H. Xia, *Acs Nano*, 3 (2009) 2653.
29. Y. Mu, H. Ming, M. Xue, F. Xian, W. Guo, H. Z. Z. Q. Shu and G. Wang, *Electrochim. Acta*, 132 (2014) 496.
30. G. Goncalves, P. A. A. P. Marques, C. M. Granadeiro, H. I. S. Nogueira, M. K. Singh and J. Grácio, *Chem. Mater.*, 21 (2009) 4796.
31. H. Tien, Y. Huang, S. Yang, J. Wang and C. C. M. Ma, *Carbon*, 49 (2011) 1550
32. R. Wang, Z. Wu, C. Chen, Z. Qin, H. Zhu, Guo. Wang, C. Wu, W. Dong, W. Fan and J. Wang, *Chem. Commun.*, 49 (2013) 8250.
33. K. Chen, L, Chen, Y, Chen, H. Bai and L. Li, *J. Mater. Chem.*, 22 (2012) 20968.
34. C. M. Welch, O. Nekrassova and R. G. Compton, *Talanta*, 65 (2005) 74.
35. L. Ding, Y. Liu, J. Zhai, A. M. Bond and J. Zhang, *Electroanal.*, 26 (2014) 121.
36. C. shan, H. Yang, D. Han, Q. Zhang, A. Ivaska and L. Niu, *Biosens. Bioelectron.*,25 (2010) 1070.
37. Z. Yan, H. Xue, K. Berning, Y. W. Lam and C. S. Lee, *Acs Appl. Mater. Inter.*, 6 (2014) 22761.
38. A. Ouejhani, M. Dachraoui, G. Lalleve and J. F. Fauvarque, *Anal. Sci*, 19 (2003) 1499.
39. M. Pettine, L. Campanella and F. J. Millero, *Environ. Sci. Technol.*, 36 (2002) 901.
40. A. Basu and B. Saha, *AJAC*, 1 (2010) 25.
41. P. M. Hallam, D. K. Kapouris, R. O. Kadara and C. E. Banks, *Analyst*, 135 (2010) 1947.
42. E. A. O. Farias, M. C. Santo, N. A. Dionísio, P. V. Quelemes, J. R. S. A. Leite, P. Eaton, D. A. Silva and C. Eiras, *Mater. Sci. Eng. B*, 200 (2015) 9.
43. S. Xing, H. Xu, J. Chen, G. Shi and L. Jin, *J. Electroanal. Chem.*, 652 (2011) 60.
44. A. Safavi, N. Maleki, and H. R. Shahbaazi, *Talanta*, 68 (2006) 1113.
45. S. Banerjee and P. Sarkar, *Sens. Lett.*, 9 (2011) 1370.